Journal of Vacuum Science & Technology B

Experimental observations and modeling of ultrashallow BF2 and As implants in single crystal silicon

A. F. Tasch, S.H. Yang, S. Morris, and D. Lim

Citation: Journal of Vacuum Science & Technology B **12**, 166 (1994); doi: 10.1116/1.587177
View online: http://dx.doi.org/10.1116/1.587177
View Table of Contents: http://scitation.aip.org/content/avs/journal/jvstb/12/1?ver=pdfcov
Published by the AVS: Science & Technology of Materials, Interfaces, and Processing

Experimental observations and modeling of ultra-shallow BF_2 and As implants in single-crystal silicon

A. F. Tasch, S.-H. Yang, S. Morris, and D. Lim
Microelectronics Research Center, Department of Electrical and Computer Engineering, Austin, Texas 78712

(Received 23 March 1993; accepted 2 August 1993)

The achievement of ultra-shallow doping profiles by ion implantation requires low energy implants and minimum thermal budgets. In this case, the profile is generally more sensitive to the implant parameters, including implant angles and dose. A detailed study has been performed of the dependence of boron and arsenic profiles on tilt angle, rotation angle, and dose for energies down to 15 keV for BF_2^+ and As^+ implants in (100) Si wafers. The major axial and planar channels have been determined using critical angle analysis and are in agreement with experimental observations. In addition, computationally efficient models have been developed for BF_2 and As implants which accurately account for the boron and arsenic profile dependence on tilt angle, rotation angle, and dose in addition to energy.

I. INTRODUCTION

The continued aggressive scaling of silicon devices to smaller feature sizes for both integrated circuits and discrete components requires more and more compact doping impurity profiles, which are almost always incorporated via ion implantation. Both lower implant energies and substantially reduced thermal processing budgets are required for achieving compact profiles with two resulting consequences. The final doping profile is more strongly controlled by the ion implant conditions such as implant angles and dose, in addition to energy; and with the use of lower implant energies, ion channeling affects a major part of the implanted impurity profile as illustrated in Fig. 1. In this figure, the large differences in arsenic concentration profiles can be seen between an arsenic implant in amorphous silicon and arsenic implants in (100) silicon at different tilt angles measured relative to the normal to the silicon surface. Thus it is highly important to understand the detailed dependence of implanted profiles on not only energy, but also on tilt angle, rotation angle (also referred to as twist or azimuthal angle), and dose. Towards this end, experimental data and/or comprehensive and accurate models are needed so that proper choices of the implant parameters may be made in order to achieve as compact a profile as possible.

Due to their high mass, arsenic and BF_2 are widely used in ion implantation to realize ultra-shallow, compact n-type and p-type profiles, respectively. In the case of the molecular species BF_2 the shallow boron profile results because of the energy partition of the boron ions when the BF_2 molecule dissociates upon entry into the silicon lattice. The effective energy of the boron ion is $\sim$11/49 of the BF_2 molecular ion energy. A similar approach using As_2^+ molecular ions has recently been reported.[1] In addition, the higher masses of arsenic and BF_2 result in more rapid damage accumulation (more rapidly reduced channeling) with increasing dose which also contributes to more compact profiles at higher doses.

Although As and BF_2 ion implantation are used commonly in the formation of ultra-shallow doping profiles, a detailed understanding of their as-implanted profile dependence on implant parameters, in particular tilt and rotation angles and dose, has not been available until recently.[2,3] In addition, current implant models for As and BF_2 which are computationally efficient and accurately account for explicit dependence on tilt angle, rotation angle, and dose in addition to energy, do not exist. Improved models are needed to accurately account for all implant parameters in one, two, and three dimensions, and they are needed to provide accurate as-implanted profile data for rapid thermal annealing diffusion modeling.

In this article, the results are reported of a detailed investigation of the dependence of arsenic and BF_2 as-implanted profiles on tilt angle, rotation angle, and dose for a range of low energies down to 15 keV. The major axial and planar channels are identified which help to guide the selection of implant parameters which provide the most compact and uniform doping profiles. These experimental data are then used to develop computationally efficient and accurate models for As and BF_2 implants which contain explicit dependence on tilt and rotation angles, dose, and energy.

II. ARSENIC IMPLANTS

Over two hundred 125 mm, (100) single-crystal silicon wafers were implanted with ^{75}As at implant energies of 15, 50, 100, and 180 keV, doses from 1×10^{13} to 8×10^{15} cm^{-2}, and a wide range of implant angles using an Eaton NV6200A ion implanter. The wafers have a thin native oxide, estimated to be $\sim$1.0 nm thick.[4] Therma-Wave maps of very low dose, high energy, normal incidence implants on two wafers out of each batch of 25 wafers were used to determine and account for the crystal cut error in the wafers.[5] The crystal cut error was found to be generally less than 0.5° for the wafers used in this study. The half-angle beam divergence of this implanter has been determined to be less than 0.5°, and tight control of the tilt and rotation angles was maintained during all implants. The implanter uses an electrostatic scanning system, which results in many different combinations of tilt and rotation angles on each wafer, with the beam entering the

 0734-211X/94/12(1)/166/6/$1.00

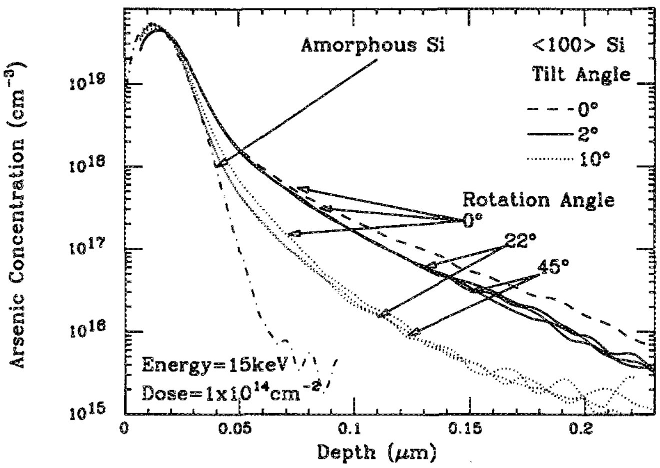

FIG. 1. Arsenic concentration profiles for As^+ implants at 15 keV measured by SIMS for various rotation angles at tilt angles of 0°, 2°, and 10° and a dose of 1×10^{14} cm^{-2}. Also shown for comparison is the profile for an implant into amorphous silicon at the same energy and dose.

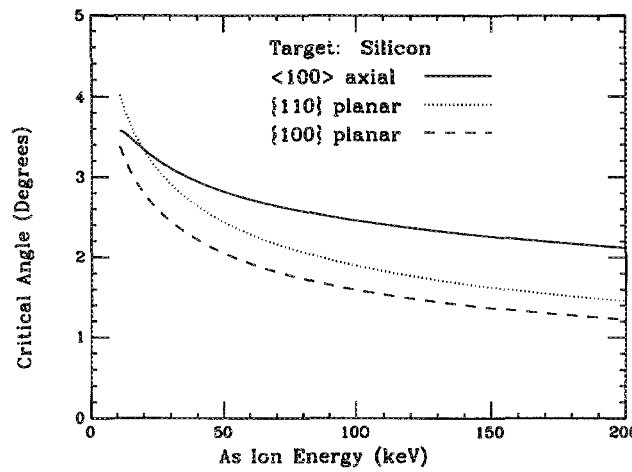

FIG. 2. Predicted critical angles for arsenic ion channeling through ⟨100⟩ axial, and {110} and {100} planar channels.

wafer at the nominal tilt and rotation angles only at the center of the wafer. At other points on the wafer surface, the implant angles are offset by an amount dependent on the configuration of the implanter and on the implant angles. The nominal implant angles were carefully chosen in order to thoroughly observe the entire angle space of 0°–10° of tilt and 0°–360° of rotation. Because of the crystal symmetry of single-crystal silicon, all possible rotation angles can be described by the rotation angles in the range of 0°–45°.

Although the profiles for all of the different energies were measured by secondary ion mass spectrometry (SIMS) and their behavior analyzed, in this article the discussion is confined to the lower energies (≤50 keV) which result in ultrashallow profiles. These profiles were measured with a single Perkin Elmer 6600 secondary ion mass spectrometer, using Cs^+ primary ion bombardment with a net impact energy of 6 keV and an incident angle of 60° from the normal to the sample surface. This energy and angle were selected based on experiments involving a range of primary ion energies in order to determine parameters that had little or no profile broadening effect. The beam current was controlled at 180 nA. The primary ion beam was rastered over an area of either (300 μm)^2, (400 μm)^2, or (500 μm)^2, depending on the sputtering rate desired. The secondary ions were collected from the central area with either 90, 120, or 150 μm on a side. The different raster sizes were required for the analysis due to the large difference in the sputtered depths which were necessary to analyze completely these implanted profiles of differing implant energies and widely varying degrees of channeling. The depths were established after the analysis by measuring the depths of the craters sputtered into the samples with a calibrated profilometer. The overall accuracy of the profiles can be expected to be within 15%.

For all implant angle combinations, the observed profiles show significant channeling tails. This indicates that, even for an implant angle combination that randomizes the incoming beam, significant secondary channeling still occurs. It is found that the effect of tilt angle is much stronger than the effect of rotation angle. The channeling dependence on tilt angle is found to be strongest near normal incidence; as the tilt angle is increased, the dependence decreases. The weaker dependence of the profile on rotation angle can only be seen at larger tilt angles where the profile has little or no dependence on tilt angle. Figure 1 shows the SIMS profiles for various rotation angles with the tilt angle fixed at 0°, 2°, and 10°. It can be seen that the effect of the tilt angle is stronger than is the case for the rotation angle.

The observed variation in the arsenic distribution profiles as the tilt and rotation angles are varied can be attributed to differences in the average distance which incoming ions travel along channels into the wafer before experiencing large angle scattering. The distance is related to the probability that the incoming ion will enter a channel in the crystal, and the ability of the channel to contain the ion over a large distance. Thus, the interpretation of the observed dependence of the As depth profiles on the tilt and rotation angles is aided by considering the critical angles for ion channeling into those channels which have a significant effect on the profile. The critical angle is defined to be the maximum angle at which an ion can approach the "potential wall" of a channel before being reflected back into the channel. This means that if an ion approaches a channel wall at an angle larger than the critical angle of the particular channel, it will break through the wall and leave the channel. An analysis of the critical angles for various axial and planar channels using an improved Si–As specific interatomic potential has been made. The calculated values of critical angles for some of the low index channels are shown in Fig. 2. Because the critical angles for higher index axial and planar channels are small compared to those for the low index channels, it is expected that channeling through only a few low index axial and planar channels contributes significantly to the total amount of channeling observed in single-crystal silicon.

From the critical angle analysis and the examination of the experimentally measured profiles, three channels have been identified as primary sources of major channeling of the incident ion beam. These are the ⟨100⟩ axial channel and two {110} planar channels. Other low index channels, such as

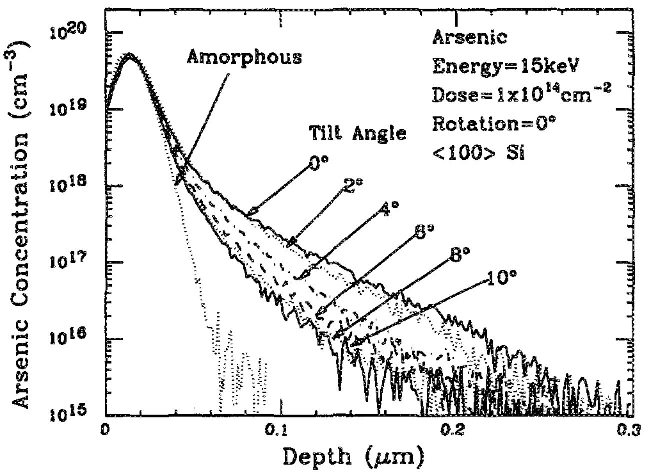

FIG. 3. Comparison of arsenic concentration profiles measured by SIMS at a fixed rotation angle of 0° and various tilt angles for a dose of 1×10^{14} cm^{-2} and an implant energy of 15 keV.

⟨110⟩ and ⟨111⟩ axial channels are not major sources of channeling in these experiments, because a tilt angle of ~45° is necessary to direct the incoming beam into these channels. As the tilt and rotation angles of the wafer are varied, the angle of the incident beam on these three channels varies. The variation in the incident angle into these low index channels results in the variation in the amount of channeling with tilt and rotation angles. Figure 3 shows the SIMS profiles resulting from 15 keV arsenic implants at 0° rotation and various tilt angles. One can see that as the tilt angle is increased through the critical angle of the ⟨100⟩ axial channel, estimated to be ~3.5° at 15 keV, the amount of channeling begins to decrease substantially.

Although 45° of rotation exposes {100} planar channels to the ion beam, no increase in channeling (or profile depth) has been observed in the range of energies studied in this work. This is believed to be due to the smaller physical size of the channel. The number and average distance of ions traveling through {100} channels is considerably less than that through {110} channels. Thus, although ions may be able to enter both channels, the effect of channeling through {110} planar channels is substantially greater than that through {100} planar channels. For this reason, this effect has not been observed within the limits of the accuracy of the SIMS data. The observed tilt and rotation angle channeling dependence is quite similar to the previously reported dependence on tilt and rotation angle for implanted boron.[2,6] A tilt angle in the range of 8°–12° and a rotation angle in the neighborhood of 45° is recommended for minimum channeling and maximum uniformity across 125–200 mm diam wafers for the energy range of 15–180 keV.

III. BF_2 IMPLANTS

For the detailed study of BF_2 implants, 180 125 mm (diameter), bare (with a thin native oxide ~1 nm thick) *p*-type (100) silicon wafers were implanted with BF_2 using the Eaton ion implanter described in the previous section. Beam currents of 7–500 μA were used, the higher beam currents being for higher dose implants to reduce the implantation time. A wafer cooling temperature of −20 °C was used, and the half-angle beam divergence of the implanter has been determined to be ~0.5°. As discussed earlier, because the Eaton NV6200A uses a fully electrostatic beam scanning method, full advantage can be taken of the variation of the actual implant angle across the wafer. That is, nominal tilt and rotation angle choices can be made so that only 6–7 wafers are required to cover the tilt angle range of 0°–10° and the complete rotation angle range of 0°–360° for each energy and dose combination. The same steps as those described in the experimental details of the arsenic implants were taken to accurately determine the ⟨100⟩ axial direction perpendicular to the wafer surface, and to achieve the highest possible degree of control of the wafer alignment during the implant. The range of implant energies and doses was 15–65 keV and 1×10^{13}–8×10^{15} cm^{-2}, respectively.

The SIMS analyses to determine the as-implanted boron profiles were performed by using a CAMECA IMS-3f ion microanalyzer. The samples were sputtered using O_2^+ primary ion bombardment with a net impact energy of 3.0 keV per O atom. This relatively low bombarding energy (and consequently greater incident angle) results in less ion beam mixing and hence improved depth resolution for the shallow as-implanted profiles. A beam current of ~1.3 μA was used, and the primary beam was rastered over areas varying from 700×700 to 350×350 μm^2. The resulting average sputter rates varied from 8.6 to 22 Å/s, respectively. The secondary ions were extracted from a 85 μm diam spot at the center of the crater. The ^{11}B signals were monitored until the background was encountered. The count rate for the B ions was converted to an equivalent concentration by using the relative sensitivity factor (RSF) determined from the measurement of ion implanted standards of known dose. The RSF is a function of the primary bombardment beam energy, and the value used in the dose quantification corresponds to the 3.0 keV effective O ion energy. The accuracy of the concentrations calculated is better than 50%. The conversion of sputtering time to depth is based on the measurement of the analytical crater depth with a Tencor stylus profilometer and is accurate to within 10%. The accuracy of the implants (including the consideration of crystal cut errors for the wafers) and the SIMS measurements were confirmed by measuring different samples from different wafers corresponding to the same implant conditions and comparing these measurements.

An analysis of the measured as-implanted boron profiles shows that for doses below the threshold dose for amorphization in BF_2^+ implanted (100) silicon (~5×10^{14} cm^{-2}), there is a significant profile variation for the boron profiles as a function of tilt angle. This is demonstrated in Fig. 4 in which the boron concentration profile is plotted for various tilt angles with the rotation angle being fixed at 0° at a fluence of 1×10^{13} cm^{-2} and with an energy of 15 keV. The rotation angle dependence of the profiles is not as strong as is the tilt angle dependence. This is illustrated in Fig. 5 where boron profiles are plotted for various rotation angles, at a tilt angle of 10°, for the same energy and dose. The tilt angle of 10° is chosen for examining the rotation angle dependence, because at this large of tilt angle, the dominant ⟨100⟩ axial channeling is minimized. As can be seen however, at 15 keV the profile

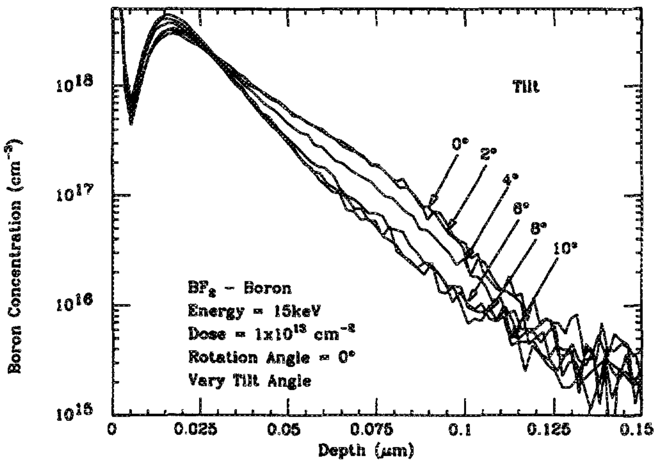

FIG. 4. Comparison of boron concentration profiles measured by SIMS for BF_2 implants at a fixed rotation angle of 0° and various tilt angles for a dose of 1×10^{13} cm^{-2} and an energy of 15 keV.

exhibits little if any dependence on rotation angle. It is necessary to go to higher energies (≥35 keV) before significant rotation angle dependence can be observed. Both the tilt and rotation angle dependence of the profiles decreases markedly as the implant dose is increased due to increased crystal damage and thus reduced channeling.

The observed variation of the boron profiles is due to the dependence of the channeled part of the profile on the implant angles and dose. In the same manner as that described for the analysis of the as-implanted As profiles, critical angle calculations and a detailed analysis of the boron profiles resulting from the BF_2 implants were performed. The results show that, similarly to As implants, the channeling takes place primarily through three channels for the tilt angle and rotation angle ranges of 0°–10° and 0°–360°, respectively. These three channels are the ⟨100⟩ axial channel and two {110} planar channels. The ⟨111⟩ and ⟨110⟩ low index axial channels have critical angles comparable to or larger than

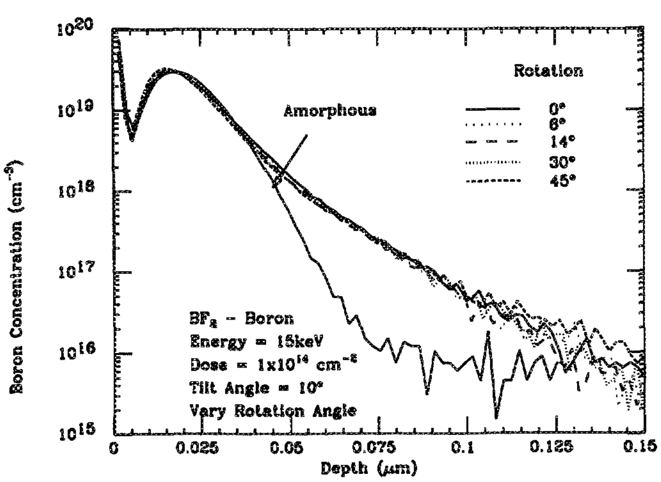

FIG. 5. Comparison of boron concentration profiles measured by SIMS for BF_2 implants at a fixed tilt angle and various rotation angles for a dose of 1×10^{14} cm^{-2} and an energy of 15 keV. Also shown for comparison is the profile for an implant into amorphous silicon at the same energy and dose.

that of the ⟨100⟩ axial channel but are not important for the range of angles used in this study. The incident ion beam would have to be incident at very large tilt angles in the vicinity of 45° in order for substantial channeling to be observed in the ⟨111⟩ and ⟨110⟩ axial channels. It should be mentioned that no channeling was detected in the {100} planar channels which, as mentioned before for the case of arsenic, is believed to be due to the relatively small physical size of the channel.

The boron profile dependence on tilt and rotation angle at the lower doses as governed by three low index channels described above is the same dependence as that observed for boron profiles formed by elemental boron implants.[2,6] This is to be expected, because the BF_2^+ ion is expected to dissociate upon entry into the silicon lattice so that the boron travels through the lattice just as in the case of the elemental boron implant but with reduced energy due to energy partitioning between the boron atom and the two fluorine atoms. For the energy range used in this study (15–65 keV), it is believed that tilt angles in the range 8°–12°, and rotation angles in the neighborhood of 45° will result in minimum channeling and maximum uniformity across 150–205 mm diam wafers.

IV. COMPUTATIONALLY EFFICIENT MODELS

In the Introduction of this article, it was pointed out that there is an important need for accurate and computationally efficient models which have explicit dependence on tilt angle, rotation angle and dose, in addition to energy. A strategy consisting of a two-prong, parallel development approach for each implanted species of interest has been used at The University of Texas at Austin. In the interest of maximum computational efficiency and easy retrofit into process modeling codes, the first part of this strategy has been to adopt a semiempirical modeling approach based on the dual-Pearson model in which the model parameters are extracted from either experimental data or from accurate physically based models which are typically more computationally intense.[7] The bimodal nature that is often observed for ion implanted impurities, led to the development of the dual-Pearson model which uses the sum of two separate Pearson functions to represent two distinct ion scattering mechanisms in crystalline solids: random scattering and channeling. As illustrated in Fig. 6, this model accurately describes the entire profile of the implanted impurity distribution and, as will be shown later, also accounts very well for the profile dependence on all of the implant parameters including dose, tilt angle, and rotation angle as well as energy. The other part of the modeling strategy has been to develop accurate physically based (not necessarily computationally efficient) models in order to provide the theoretical foundation required for technology development and process control, and to serve as much as possible as the basis for the computationally efficient semiempirical models. Space does not permit a discussion of the Monte Carlo, physically based models that have been developed, but a detailed description can be found in Refs. 8 and 9.

In the development of the computationally efficient dual-Pearson models for BF_2 and As implants, model parameters were extracted from over 400 SIMS boron profiles of BF_2^+

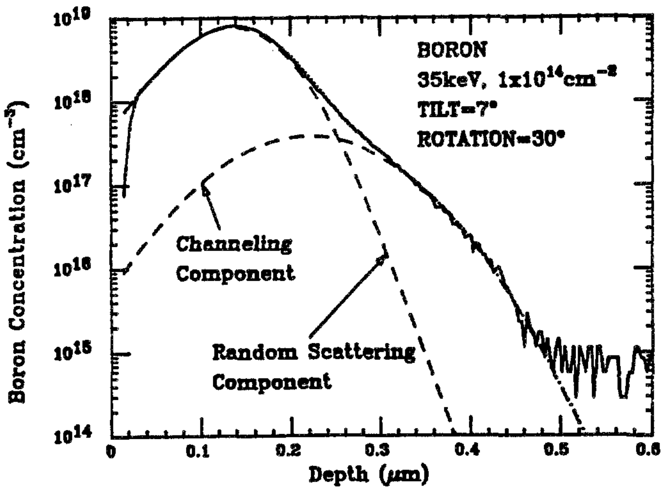

FIG. 6. Illustration of the dual-Pearson semiempirical model.

implants, and over 400 SIMS arsenic profiles of As^+ implants. For each profile, nine parameters were extracted for the dual-Pearson model, and in order to rapidly extract this very large number of parameters, a user-friendly, fully automatic parameter extraction code (DUPEX) was developed.[10] In this code, a trial set of parameters is automatically generated by the software in the first step, and this trial set is used as the initial guess for the second step, the least-squares fitting with the Levenberg–Marquardt algorithm.[11,12] In order to demonstrate the features of these new comprehensive and computationally efficient implant models, the models, along with the extracted modeling parameters as a function of energy, dose, and tilt and rotation angles, and new code have been implemented in SUPREM 3.[13] Tilt and rotation angles were added as new options to the implant statement in SUPREM 3. A four-step interpolation algorithm was developed in order to accurately and efficiently interpolate between look-up table values of the nine dual-Pearson parameters when the specified implant conditions do not exactly match the experimentally determined implant parameters.

Simulated profiles for boron and arsenic using these new models are compared with experimentally measured profiles in Figs. 7 and 8. The dependence on tilt angle is examined in Fig. 7, while the dose dependence is compared in Fig. 8. As can be seen, the dual-Pearson model is able to very accurately predict the experimentally observed dependence. It should be noted that the discrepancy between the predicted and measured boron profiles in the top 150 A of the silicon surface in Figs. 7(a) and 8(a) is due to surface contamination and transient effects in the SIMS measurements. The actual profiles in this region are believed to be more accurately represented by the simulated curves.

The accuracy of the dual-Pearson, computationally efficient model for arsenic and BF_2 implants has been illustrated for 15 keV implants in this article, because of the interest and focus on ultra-shallow doping profiles in this International Workshop. The model has demonstrated an equally high degree of accuracy for both BF_2 and As implants for the range of implant parameters listed in the previous sections of this

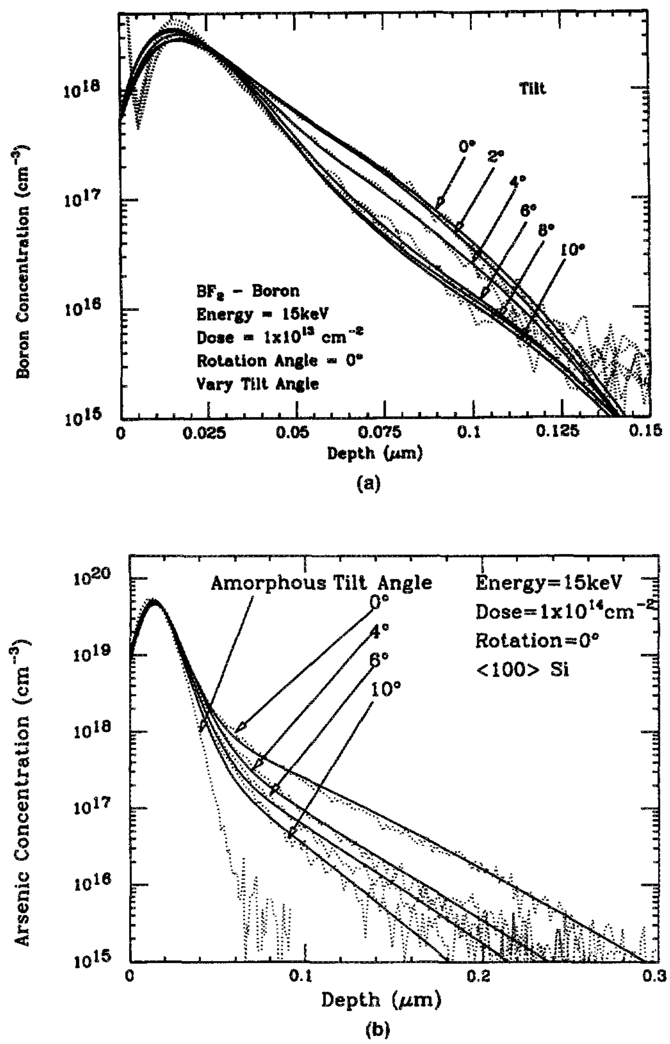

FIG. 7. Examples of profile simulations using the new dual-Pearson model for (a) boron profiles resulting from BF_2 implants and (b) arsenic profiles resulting from As implants. The solid curves are the simulations, and the dotted curves represent the experimentally measured profiles. The variation of the profiles with tilt angle is very accurately predicted.

article.[14,15] The range of implant parameters in the currently implemented models in SUPREM are

BF_2: 15–65 keV, 0°–10° tilt angle,
0°–360° rotation angle,
and any dose up to 10^{16} cm^{-2}

As: 15–180 keV, 0°–10° tilt angle,
0°–360° rotation angle,
and any dose up to 10^{16} cm^{-2}.

Although these models have not been tested at doses above 10^{16} cm^{-2}, they are believed to be able to faithfully represent higher doses. Finally, it should be mentioned that a computationally efficient model based on the dual-Pearson approach has also been developed for elemental boron implants for the following range of parameters: 15–80 keV, 0°–10° tilt angle, 0°–360° rotation angle, and any dose up to 10^{16} cm^{-2}.[16]

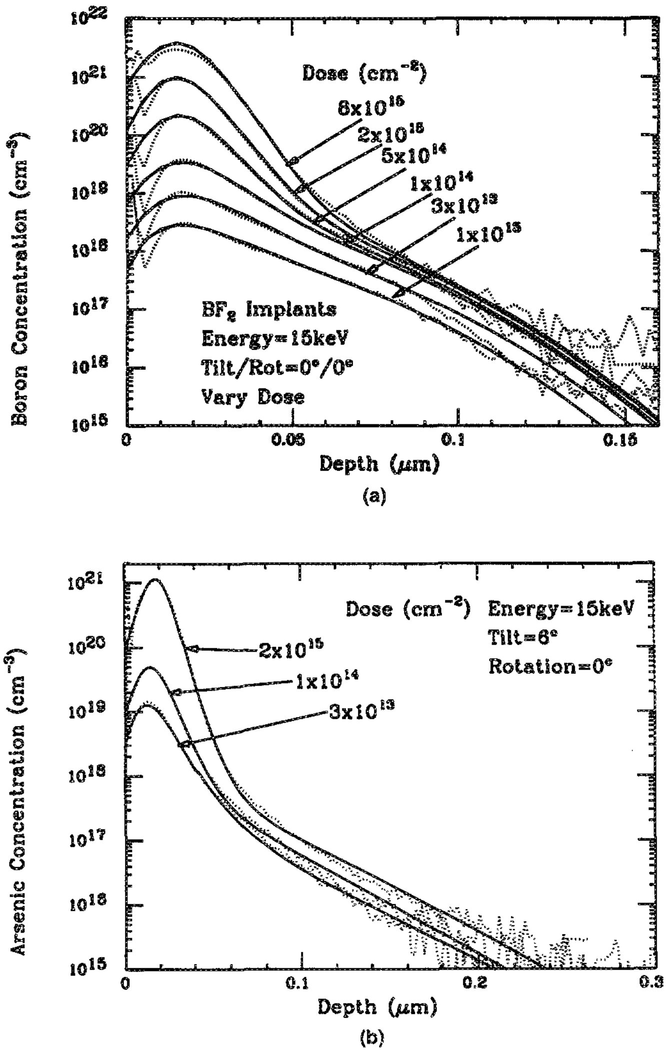

FIG. 8. Examples of profile simulations using the new dual-Pearson model for (a) boron profiles resulting from BF_2 implants and (b) arsenic profiles resulting from As implants. The solid curves denote the simulated profiles, and the dotted curves represent the experimentally measured profiles. The variation of the profiles with dose is very accurately predicted.

V. CONCLUSIONS

The successful application of As and BF_2 ion implantation for the formation of ultra-shallow doping profiles requires a comprehensive understanding of the concentration profile dependence on key implant parameters such as tilt and rotation angles and dose, in addition to energy. This article has described the results of a very detailed study to obtain that understanding. For the ranges of energies examined for BF_2 and As, the profile dependence is governed by channeling through three major channels, the ⟨100⟩ axial channel and two {110} planar channels. The amount of channeling is strongest at low tilt angles ($\leqslant 5°$) and weakly dependent on the {110} planar channels, especially at the lower implant energies. The nonchanneled part of the profile increases rapidly with dose at moderate and higher doses due to the rapid increase in lattice damage by these heavier mass species.

Comprehensive and computationally efficient models have been developed for BF_2 and As implants for the range of implant parameters considered in this study. These models allow profile optimization in technology development and an understanding of the profile dependence on the implant parameters in the development of process control strategies in manufacturing. Finally, these models provide accurate as-implanted concentration profile data for rapid thermal annealing diffusion modeling.

ACKNOWLEDGMENTS

This work was supported in part by SEMATECH, the Semiconductor Research Corporation, Intel, and Motorola.

[1]B. G. Park *et al.*, IEEE Electron Device Lett. **EDL-13**, 507 (1992).
[2]K. M. Klein *et al.*, J. Electrochem. Soc. **138**, 2102 (1991).
[3]S.-H. Yang, *Proceedings of the Symposium on Phase Formation and Modifications by Beam–Solid Interactions*, 1991 Fall Meeting of the Materials Research Society (Materials Research Society, Pittsburgh, PA, 1991).
[4]P. A. M. van der Heide *et al.*, *The Electrochemical Society of Extended Abstracts* (Electrochemical Society, Pennington, NJ, 1989), Vol. 89-2, p. 604.
[5]W. L. Smith *et al.*, Solid State Technol. **29**, 85 (1986).
[6]C. Park *et al.*, J. Electrochem. Soc. **138**, 2107 (1991).
[7]A. F. Tasch *et al.*, J. Electrochem. Soc. **136**, 810 (1989).
[8]K. M. Klein *et al.*, *1991 IEEE International Electron Devices Meeting Technical Digest* (IEEE, New York, 1991), p. 697.
[9]K. M. Klein *et al.*, IEEE Trans. Electron Devices **ED-39**, 1614 (1992).
[10]C. Park *et al.*, Solid-State Electron. **33**, 645 (1990).
[11]K. Levenberg, Quart. Appl. Math. **2**, 164 (1944).
[12]D. Marquardt, SIAM J. Appl. Math. **11** 431 (1963).
[13]C. P. Ho *et al.*, IEEE Trans. Electron. Devices **ED-30**, 1438 (1983).
[14]S. J. Morris *et al.*, *Electrochemical Soc. Extended Abstracts* (Electrochemical Society, Pennington, NJ, 1992), Vol. 92-1, p. 450.
[15]S.-H. Yang (unpublished).
[16]C. Park *et al.*, COMPEL **10**, 331 (1991).